Finite-size scaling in the ***p***-state mean-field Potts glass: exact statistical mechanics for small samples

1996 J. Phys. A: Math. Gen. 29 3503

(http://iopscience.iop.org/0305-4470/29/13/020)

J. Phys. A: Math. Gen. **29** (1996) 3503–3519. Printed in the UK

Finite-size scaling in the p-state mean-field Potts glass: exact statistical mechanics for small samples

B O Peters†, B Dünweg, K Binder, M d'Onorio de Meo and K Vollmayr
Institut für Physik, Johannes Gutenberg-Universität, KoMa 331, D-55099 Mainz, Germany

Received 30 October 1995, in final form 16 February 1996

Abstract. The mean-field Potts glass with bimodal bond distribution is studied, for $p = 3$ and $p = 6$ Potts states, via exact summation of the partition function of systems of up to $N = 15$ sites. Averages over the disorder realizations are also done exactly up to $N = 8$, while random bond configurations are generated for the larger systems. Our enumeration method is described in some detail, and the applicability of finite-size scaling (FSS) for our very small systems is discussed. For $p = 3$ (second-order transition), the data agree reasonably with the FSS relations given by Parisi *et al* for the $p = 2$ (Ising) case. For $p = 6$, no clear signs of the predicted first-order behaviour could be observed. This case is even more affected by finite-size effects, since the necessary antiferromagnetic bias of the bond distribution introduces an additional N^{-1} correction in the free energy. For both p, the data are compatible with a vanishing ground-state entropy.

1. Introduction

Spin glasses are model materials suitable to elucidate new glass-like phases and show new ordering phenomena in disordered solids [1–4]. Research in this area has even stimulated progress in quite different fields such as optimization problems, neural networks, etc [4].

A generalization of the Ising spin glass to a model with p discrete states, $s_i \in \{1, \ldots, p\}$, is the Potts glass (PG) [5–8]. An exchange energy J_{ij} between these Potts spins arises only if the considered pair (i, j) of sites occurs in the same state. This model can be considered as a generic model of anisotropic orientational glasses [9], if we associate the p discrete states with p orientations of a uniaxial molecule in the crystal. (Orientational glasses result from random dilution of molecular crystals, e.g. N_2 diluted with Ar.) Thus, $p = 3$ if the molecules can align only along the x, y, z axes of a cubic crystal, while $p = 6$ if they can align along the face diagonals.

The main interest in this model does not stem from the application to these materials, however, but from some properties found for the *infinite range* version of the model. The transition from the paramagnetic to the spin-glass phase is here of second order for $p \leqslant 4$ but of first order for $p > 4$. Although in the latter case the glass order parameter at the transition appears discontinuously, there is no latent heat [6]. In addition, at lower temperature a further transition occurs—presumably to a randomly canted 'ferromagnetic' phase (RCFM), but very little is actually known about this second transition and the associated low-temperature phase. Finally, we mention that the dynamic variant of the mean-field theory of Potts glasses [10, 11] shows a number of similarities to the mode-coupling theory of the structural glass transition [12].

† Present address: Forschungszentrum KFA, HLRZ, D-52425 Jülich, Germany.

0305-4470/96/133503+17$19.50

In order to understand all these properties in more detail, one would like to know whether these puzzling features are just peculiarities of the infinite interaction range limit or also survive for short-range models, and if so, for which spatial dimensionalities d. In fact, estimates for the upper critical dimension d_u (for $d > d_u$ mean-field theory should hold) range from $d_u = 6$ [1, 9] to $d_u = 8$ [13]. In contrast, a Monte Carlo (MC) work for a nearest-neighbour PG in $d = 4$ with $p = 3$ states [14] has been interpreted as being compatible with a first-order glass transition. However, these studies were made for extremely small systems and hence are plagued with finite-size effects, which are not well understood. Before any firm conclusions can be drawn, an investigation of finite-size effects on such unconventional transitions is mandatory. As a matter of fact, a study of the finite-size effects in the infinite-range Ising spin glass has already provided important checks of the theory [15, 16], and it is likely that a study of size effects for the infinite range Potts glass might be similarly useful.

As a first step in this direction, we start in the present paper by a discussion of the statistical mechanics of very small systems for which the partition function can be exactly enumerated. Although this approach is limited to extremely small samples, experience with the Ising case [15] has demonstrated its usefulness and feasibility, since it yields precise results. Additionally, the computation of the partition function is not hampered by the problem of critical slowing down, which is so cumbersome in the MC studies [1, 9], and easily yields data for a large range of temperatures down to the ground state. Even in cases where such results do not yet allow an unambiguous extrapolation to the thermodynamic limit, they are useful as a test of the accuracy of standard MC work.

In the next section, we define the model and most of the quantities that are calculated, and discuss the behaviour of the model in the high-temperature limit. The computational methods needed to make the problem tractable are also described in section 3. Section 4 then presents a finite-size scaling analysis, inspired by the treatment of Parisi *et al* [16]. Both the case $p = 3$ and the case $p = 6$ are presented, and the entire range of temperatures is discussed including ground-state properties and the specific heat behaviour. The last section gives a summary of our results.

2. The model

We study the mean-field Potts glass Hamiltonian of N interacting Potts spins $s_i \in \{1, \ldots, p\}$ on sites $i \in \{1, \ldots, N\}$,

$$\mathcal{H} = -p \sum_{i<j} J_{ij} \delta_{s_i s_j} \tag{1}$$

where p is the number of Potts spin states, and the J_{ij} are random quenched interaction constants (bonds) with mean $J_0 \equiv [J_{ij}] \equiv \tilde{J}_0/(N-1)$ and variance $(\Delta J)^2 \equiv [J_{ij}^2] - [J_{ij}]^2 \equiv \tilde{J}^2/(N-1)$, where we use $[\cdots]$ to denote an average over the disorder realizations. The 'thermodynamic' (i.e. system-size independent) parameters are $\tilde{J}$ and $\tilde{J}_0$; this scaling of the interactions with the system size is necessary in order to ensure proper extensivity of the system with $\frac{1}{2}N(N-1)$ equivalent bonds. While analytical calculations usually assume a Gaussian distribution of bonds,

$$P_G(J_{ij}) = \frac{1}{\sqrt{2\pi}(\Delta J)} \exp\left\{-\frac{(J_{ij} - J_0)^2}{2(\Delta J)^2}\right\}$$

we here use, for computational simplicity, the bimodal distribution

$$P_b(J_{ij}) = x\delta(J_{ij} - J) + (1-x)\delta(J_{ij} + J)$$

with $J = \sqrt{J_0^2 + (\Delta J)^2}$ and $x = \frac{1}{2}(1 + J_0/J)$. Although this distribution differs considerably from a Gaussian, we can nevertheless compare our data to the results which have been obtained for the model in the thermodynamic limit. In this limit, only the first two moments will matter, and it has even been shown that the first-order corrections to FSS will coincide [16]. As usual, we introduce the simplex spin representation [17] such that the state s_i corresponds to a $(p-1)$-dimensional unit vector $\vec{S}_i$ pointing into the ith corner of a p-simplex, i.e.

$$\vec{S}_i \cdot \vec{S}_j = \frac{p\delta_{s_i s_j} - 1}{p-1} .$$

The temperature is given in units of $\tilde{J}/k_{\mathrm{B}}$, i.e. we set $\tilde{J} = k_{\mathrm{B}} = 1$. In these units, the system undergoes a phase transition from the paramagnetic (PM) to a spin glass (SG) phase at the critical temperature $T_c = 1$. At a second temperature $T_2 = (p/2-1)/(1-\tilde{J}_0)$ another phase transition to a randomly canted ferromagnetic phase [5, 7] occurs, and hence the spin-glass phase is limited to the temperature range $T_2 < T < T_{\mathrm{c}}$, and would not exist at all if $T_2 > T_{\mathrm{c}}$, i.e. if $\tilde{J}_0 > 2 - p/2$. For $p > 4$, this value is negative, i.e. in this case a certain amount of antiferromagnetism is needed in order to stabilize the spin-glass phase. We have always used $\tilde{J}_0 = 3 - p$ such that $T_2 = \frac{1}{2}$.

2.1. The order parameter

The natural magnetic order parameter in the Potts model is

$$m \equiv \sqrt{\sum_{\mu=1}^{p-1} m_\mu^2} \tag{2}$$

where the m_μ denote the $p-1$ components of the simplex magnetization

$$\vec{m} \equiv \frac{1}{N} \sum_{i=1}^{N} \vec{S}_i .$$

We will denote the kth moment of the magnetization distribution by $M^{(k)} \equiv [\langle m^k \rangle]$, using the standard notation $\langle \cdots \rangle$ for the thermal average at fixed bond configuration. Following [18–21], the spin-glass order parameter q is defined via

$$q \equiv \sqrt{\sum_{\mu,\nu=1}^{p-1} (q^{\mu\nu})^2} \tag{3}$$

where

$$q^{\mu\nu} \equiv \frac{1}{N} \sum_{i=1}^{N} S_{i,1}^{\mu} S_{i,2}^{\nu} \tag{4}$$

defines a tensor of overlap parameters taken between two replicas 1 and 2, the latter being defined as thermally independent systems with identical realization of the disorder. Only even moments can be evaluated easily, since then the square root in (3) does not occur, and we can exploit the statistical independence of the two replicas. However, in each replica, the thermal averages are the same, since these are averages over the *full* configuration space of the finite system, such that ergodicity breaking, or replica-symmetry breaking, cannot

occur. Hence, it is sufficient to consider only one system. For example, one finds for the second moment, which is directly related to the spin-glass susceptibility χ_{SG},

$$q^{(2)} \equiv [\langle q^2 \rangle] = \frac{1}{N^2} \sum_{i,j} [\langle \vec{S}_i \cdot \vec{S}_j \rangle^2] = \frac{1}{N} \chi_{\mathrm{SG}}$$

where we have used the relations

$$\langle S^{\mu}_{i,1} S^{\nu}_{i,2} S^{\mu}_{j,1} S^{\nu}_{j,2} \rangle = \langle S^{\mu}_{i,1} S^{\mu}_{j,1} \rangle \langle S^{\nu}_{i,2} S^{\nu}_{j,2} \rangle$$

i.e. the statistical independence of the replicas, and

$$\langle \vec{S}_{i,1} \cdot \vec{S}_{j,1} \rangle = \langle \vec{S}_{i,2} \cdot \vec{S}_{j,2} \rangle$$

i.e. their equivalence. The analogous formula for the fourth moment is

$$q^{(4)} = \frac{1}{N^4} \sum_{i,j} \sum_{k,l} [\langle (\vec{S}_i \cdot \vec{S}_j)(\vec{S}_k \cdot \vec{S}_l) \rangle^2]. \tag{5}$$

For reasons of computational complexity, we did not study any higher moments. For $p = 6$, we found ourselves unable to even evaluate $q^{(4)}$. Usually, the fourth moment is used in order to obtain the fourth-order cumulant g_4 which we normalize here according to

$$g_4 \equiv \frac{(p-1)^2}{2} \left(1 + \frac{2}{(p-1)^2} - \frac{q^{(4)}}{(q^{(2)})^2} \right).$$

This convention follows [22], which studied the behaviour of the analogous quantity for pure Potts models near a first-order transition. The parameter $(p-1)^2$ occurs as the order parameter dimensionality, which is, in our case, the number of tensor components.

The nature of the phase transitions has been analysed by Elderfield *et al* [5], Gross *et al* [6], and Cwilich *et al* [7]: for $p < 4$ the transition PM to SG is continuous, while for $p > 4$ the transition has no latent heat but a discontinuity in the order parameter [7], which jumps from zero to a finite value q_{jump}, which is, in leading order of a $(p-4)$ expansion,

$$q_{\mathrm{jump}} = \frac{2(4-p)}{p^2 - 18p + 42} \tag{6}$$

in our units. (This formula yields $q_{\mathrm{jump}} = \frac{2}{15} \approx 0.13$ for $p = 6$.) At $T < T_2 = 0.5$, the SG phase becomes unstable, and the system goes into a more complicated spin-glass phase, where the shape of Parisi's [23] order parameter function $q(x)$ is more complicated. This low-temperature phase has been called a 'randomly canted ferromagnetic phase' (RCFM), since the order parameters parallel and vertical to an external field in the zero-field limit are no longer equal.

2.2. High-temperature behaviour

It is straightforward to calculate the leading-order terms of the high-temperature series expansion of the free energy per site, since at infinite temperature the averages over the spin configurations and the disorder decouple. We found up to linear order in $\beta = 1/T$

$$\begin{aligned} \frac{F}{N} &= -(\beta N)^{-1} \left[\ln \sum_{\{s_i\}} \exp(-\beta \mathcal{H}) \right] \\ &= -\beta^{-1} \ln p - \frac{\tilde{J}_0}{2} - \frac{\beta}{4}(p-1) \left(\tilde{J}^2 + \frac{\tilde{J}_0^2}{N-1} \right) + \cdots . \end{aligned}$$

From this, one readily obtains for the entropy per site

$$\frac{S}{N} = \ln p - \frac{\beta^2}{4}(p-1)\left(\tilde{J}^2 + \frac{\tilde{J}_0^2}{N-1}\right) + \cdots$$

and for the internal energy per site

$$\frac{U}{N} = -\frac{\tilde{J}_0}{2} - \frac{\beta}{2}(p-1)\left(\tilde{J}^2 + \frac{\tilde{J}_0^2}{N-1}\right) + \cdots$$

showing that for non-vanishing first moment of the bond distribution there is a considerable finite-size effect in these quantities, even up to rather large temperatures.

For the spin observables we did not evaluate the finite-T corrections. For the second moment of the magnetization one finds $[\langle m^2\rangle_{T=\infty}] = N^{-1}$, while the other moments scale trivially with N in direct analogy to a random walk, $[\langle m^k\rangle_{T=\infty}] \propto N^{-k/2}$. For the glass order parameter moments one finds $q^{(2)}_{T=\infty} = N^{-1}$ and

$$q^{(4)}_{T=\infty} = \frac{1}{N^2}\left(1 + \frac{2}{(p-1)^2}\frac{N-1}{N}\right)$$

such that the fourth-order cumulant at $T = \infty$ has simply the value $g_4 = N^{-1}$ for every p.

3. Computational method

Our main interest was to study the FSS of the phase transitions as well as the ground state behaviour in the Potts glass. Different methods are available: Monte Carlo (MC) simulation, replica field theory, and the calculation of the exact partition function. In order to be unaffected by large relaxation times at $T \to 0$ and $T \to T_c$ [24, 25], and since the replica field method has already been explored thoroughly [16, 26], we decided to investigate the PG by computing the exact partition function. A particular advantage of this approach is the fact that all temperatures from $T = 0$ to $T = \infty$ are available from a single run. The computation is complex, but feasible if one exploits the symmetries of the model.

3.1. Computational complexity

The thermal average of an observable $A = A_{\{J_{ij}\}}(\{s_i\})$ reads

$$\langle A\rangle = \frac{1}{Z}\sum_{\{s_i\}} A(\{s_i\})\mathrm{e}^{-\beta\mathcal{H}} \tag{7}$$

where $Z = \sum_{\{s_i\}} \mathrm{e}^{-\beta\mathcal{H}}$ is the partition function. The number of elements in the sum (7) is the number of spin configurations: $\#\{\{s_i\}\} = p^N$. Hence, without optimization the necessary CPU time for a single bond configuration would already increase exponentially with N. The bond average, when done exactly, scales even worse, since the number of bond configurations is $2^{N(N-1)/2}$, increasing faster than exponentially with N. However, for both summations the computational complexity can be reduced considerably, as outlined below.

3.2. Optimizations

(i) *Bit coding.* The exponent in the Boltzmann factor reads

$$-\beta\mathcal{H} = +\beta p\sum_{i<j} J_{ij}\delta_{s_i s_j}.$$

Writing

$$J_{ij} = J(\delta_{J_{ij},+J} - \delta_{J_{ij},-J}) \equiv J(g_{ij}^{+} - g_{ij}^{-})$$

and introducing $\tilde{\beta} \equiv \beta p J$, the exponent may be separated into a real part and an integer part where the summation takes place:

$$-\beta\mathcal{H} = \tilde{\beta} \sum_{i<j} (g_{ij}^{+} - g_{ij}^{-}) \delta_{s_i s_j}.$$

Defining a vector notation

$$\vec{J} \equiv (J_{12}, J_{13}, J_{14}, \ldots, J_{1N}, J_{23}, J_{24}, \ldots, J_{2N}, J_{34}, \ldots, J_{N-1,N})$$

(similarly for $\vec{\delta}$, $\vec{g^{+}}$, and $\vec{g^{-}}$), the exponent can be rewritten as

$$-\beta\mathcal{H} = \tilde{\beta}(\vec{g^{+}} \cdot \vec{\delta} - \vec{g^{-}} \cdot \vec{\delta}) .$$

The vectors $\vec{\delta}$, $\vec{g^{+}}$ and $\vec{g^{-}}$ were stored in bit arrays in order to save memory and to calculate the scalar products in a more efficient way, using logical bit functions.

(ii) *Equivalent spin configurations*. As a consequence of the Potts symmetry, several (at least p, at most $p!$) spin configurations belong to the same δ-vector. By constructing a histogram $n(\vec{\delta})$, and evaluating the sum (7) only for different δ-vectors, the computation time can be reduced by a factor of roughly $p!$ The partition function then is

$$Z = \sum_{\{s_i\}} \mathrm{e}^{-\beta\mathcal{H}} = \sum_{\vec{\delta}} n(\vec{\delta}) \mathrm{e}^{-\beta\mathcal{H}} .$$

However, the histogram $n(\vec{\delta})$ is rather large (it contains roughly $p^N/p!$ entries), resulting in a non-trivial memory requirement which limits the feasible system size considerably.

(iii) *Density of states*. Ferrenberg and Swendsen [27] promoted a histogram method for Monte Carlo simulations. At a certain inverse temperature β_0, the microcanonical partition function $\Omega(E)$ (i.e. the number of states having a certain energy E) is estimated. Thermal averages of observables $f = f(E)$, which only depend on the energy, are then evaluated for temperatures $\beta \approx \beta_0$. Due to statistical errors in $\Omega(E)$, the temperature region of the extrapolation is limited. However, in the present method we enumerate $\Omega(E)$ exactly, and thus $\langle f(E) \rangle$ can be evaluated for *all* temperatures. The gain in efficiency is rather obvious: knowledge of $\Omega(E)$ enables us to use the identity

$$\sum_{\{s_i\}} f(\mathcal{H}(\{s_i\})) \mathrm{e}^{-\beta\mathcal{H}(\{s_i\})} = \sum_{E} \Omega(E) f(E) \mathrm{e}^{-\beta E} .$$

The sum on the left-hand side contains p^N terms, whereas the right-hand side scales only with N^2. Similarly, we used an analogous approach for calculating magnetization and order-parameter moments.

With the help of these optimization steps, the computation of all observables for all temperatures and one disorder realization took about one minute on an IBM RISC6000 workstation, for either ($N = 15$, $p = 3$) or ($N = 12$, $p = 6$). (Without any optimization, this computation would have lasted several years.)

(iv) *Equivalent bond configurations*. For the exact disorder average, which turned out to be feasible up to $N = 8$ (i.e. 2^{28} bond configurations), we took advantage of a permutation symmetry which reads: *two bond configurations* $\{J_{ij}\}$ *are equivalent (i.e. in particular, will yield the same thermodynamic averages) if there is a permutation of the indices* i, j *transferring one configuration into the other*. This problem is straightforwardly mapped to graph theory [28] by simply noting that a line connecting two points can be associated with

a $+J$-bond, while a non-existing line between the points corresponds to a $-J$-bond, such that every bond configuration can be uniquely identified with a graph.

In order to exploit this symmetry, one needs to know all the equivalence classes of graphs and the number of graphs within a given equivalence class. The disorder average can then be replaced by a weighted average over equivalence classes. Within a class it is sufficient to do the calculation for just one arbitrarily chosen bond configuration, a class representative. This is a very important optimization step, since the number of classes is *substantially* smaller than the number of bond configurations.

However, in the literature [28] one finds only the total number of equivalence classes, without any information on their individual sizes, and that only for small N. In order to distinguish between graphs of different classes, one has to find a number g_i attributed

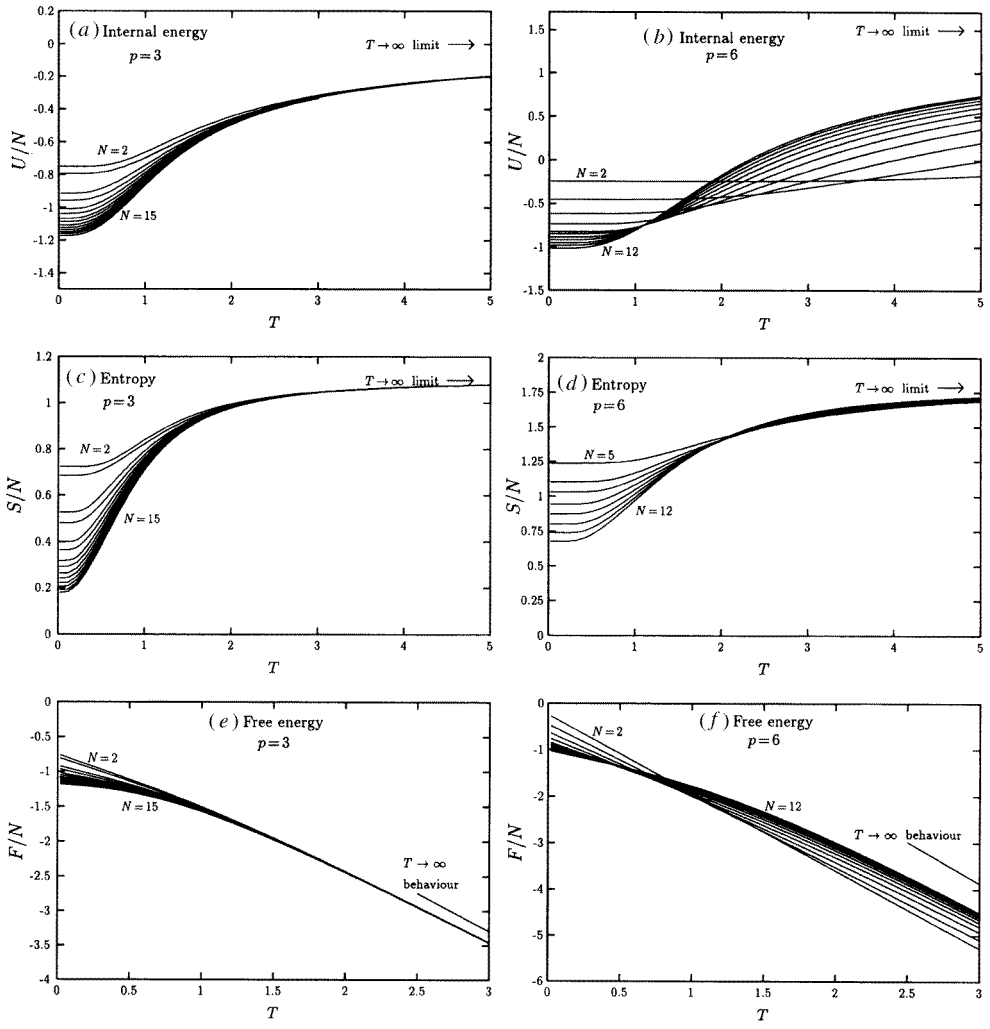

Figure 1. Internal energy per spin U/N (a) for $p = 3$ and (b) $p = 6$, entropy per spin S/N for (c) $p = 3$ and (d) $p = 6$ and free energy per spin F/N (e) for $p = 3$ and (f) $p = 6$ plotted versus temperature.

to graph i, with $g_i = g_j$ if i and j are equivalent, but $g_i \neq g_j$ if they are not. We tried to satisfy this property by choosing a simple but sufficiently complex observable—the thermally averaged square of the magnetization in the $p = 3$ states Potts glass $\langle \vec{m}^2 \rangle$, which was computed for every single-bond configuration at a non-trivial, fixed temperature $T = 1$. The numerical effort needed for this average is small compared to that which would be needed to calculate more complicated quantities like $q^{(2)}$ and $q^{(4)}$ in the same way, and therefore a 'preliminary' calculation of $\langle \vec{m}^2 \rangle$, which also yields information on the degeneracies, is very useful. In order to obtain the latter, we counted the number of occurrences of $\langle \vec{m}^2 \rangle$, i.e. we constructed a histogram, considering two bond configurations as equivalent if they yielded the same value of $\langle \vec{m}^2 \rangle$, and without checking if they could actually be mapped onto each other by a permutation. For $N \leqslant 7$, the number of generated $\langle \vec{m}^2 \rangle$ values was found to be exactly equal to the number of equivalence classes known from [28]. This means, of course, that there is a one-to-one correspondence between $\langle \vec{m}^2 \rangle$ values and equivalence classes, such that the size of each class is just given by the corresponding histogram value. However, it may also happen that two *different* classes 'accidentally' yield the same magnetization value, and then the number of classes will exceed the number of magnetizations. This actually occurred for $N = 8$, where we found only 12 338 different magnetizations, while there are [28] 12 346 different graph classes. Since this degeneracy, however, pertains to all observables which depend only on energy and/or magnetization (in particular, the free energy), only the q-moments can be affected. For this latter case, we decided to neglect the (obviously small) error.

For $N \geqslant 9$, the procedure turned out to be computationally too expensive; in this case we generated a large random sample of 10^5–10^6 bond configurations.

As an example, figure 1 presents our results for the free energy, internal energy and entropy of both models ($p = 3$ and $p = 6$) as a function of temperature. It is seen that for $p = 3$ the convergence to the thermodynamic limit ($N \to \infty$) is fairly smooth and rapid on the temperature scale shown. Only for about $T < 2$ are there pronounced finite-size effects, which we shall attempt to analyse in the next section. Conversely, for $p = 6$ the approach to the limiting behaviour is distinctly slower, as expected from the high-temperature expansion (cf the preceding section; note that $\tilde{J}_0 = 0$ for $p = 3$ but not for $p = 6$).

4. Numerical results

4.1. Critical behaviour for $p = 3$

The $p = 3$ PG has a continuous phase transition at $T_c = 1$, very much like the $p = 2$ case, i.e. the Sherrington–Kirkpatrick (SK) model [29, 30]. We expect the same FSS relations in both cases, with only the prefactors being different. We concentrate on the behaviour of the order parameter first.

A useful guidance about the pertinent FSS exponents is obtained from a primitive Landau theory. Starting from the usual Landau free energy per site for spin glasses [31],

$$f(q) = \frac{r}{2}q^2 + \frac{u}{6}q^3$$

where $r \propto (T - T_c)$ and $u > 0$, we use the ansatz for the probability distribution of the order parameter

$$P(q) = \frac{\mathrm{e}^{-\beta N f(q)}}{\int \mathrm{d}q\, \mathrm{e}^{-\beta N f(q)}}.$$

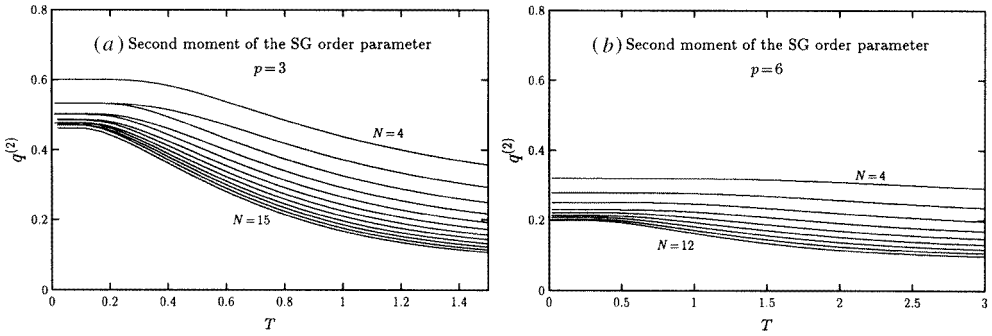

Figure 2. Second moment $q^{(2)} \equiv [\langle q^2 \rangle]$ of the spin-glass order parameter plotted versus temperature for (a) $p = 3$ and (b) $p = 6$.

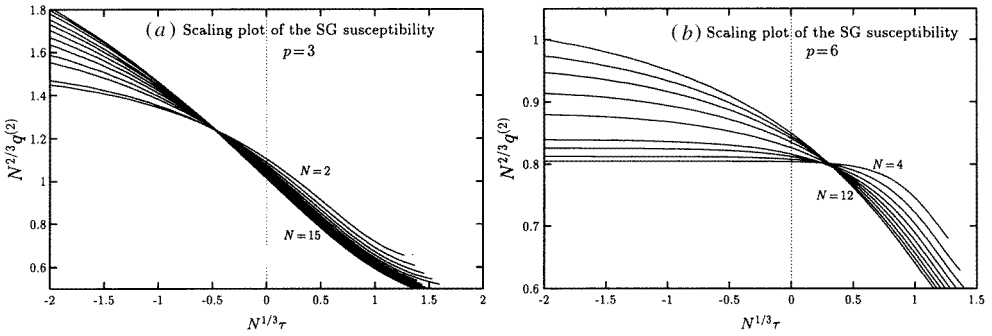

Figure 3. Scaling plot of the spin-glass susceptibility, i.e. $N^{2/3}q^{(2)}$ is plotted versus $N^{1/3}\tau$ (where $\tau = 1 - 1/T$) (a) for $p = 3$ and (b) $p = 6$. Note that we expect the data to collapse on a single curve only in the case $p = 3$ (second-order phase transition), in the asymptotic limit $N \to \infty$.

Of course, we do not expect this to really be a valid description of the physics, since one has to take into account the replicas [16]; however, the replica field theory has a quite similar structure such that the simple theory should yield the correct exponents, and the order parameter moments should, in the vicinity of T_c, scale like

$$q^{(k)} \equiv [\langle q^k \rangle] \equiv \int \mathrm{d}q \; P(q) q^k = N^{-k/3} \tilde{f}_k(N^{1/3}\tau) \tag{8}$$

where $\tilde{f}_k(x)$ are scaling functions, and $\tau \equiv 1 - 1/T$. Figure 2 shows the temperature variation of the second moment of the order parameter, and figure 3 replots the data in scaled form. However, for these small values of N there is no good 'data collapsing' yet seen, i.e. pronounced corrections to scaling occur.

The cumulant g_4 should, at T_c, not depend on N at all, since there the scaling argument vanishes and the prefactors $N^{-k/3}$ cancel out, i.e. for large enough N all curves $g_4(T)$ should intersect at one universal point. This property has found widespread application in the FSS analysis of second-order phase transitions in pure systems, in particular for the determination of T_c [32].

For impure systems like the PG the cumulant is also applied [33–36], but it is less well understood (as is FSS in general for spin glasses). For our data, no intersection point is observable, see figure 4; we attribute this behaviour to strong corrections to scaling and to

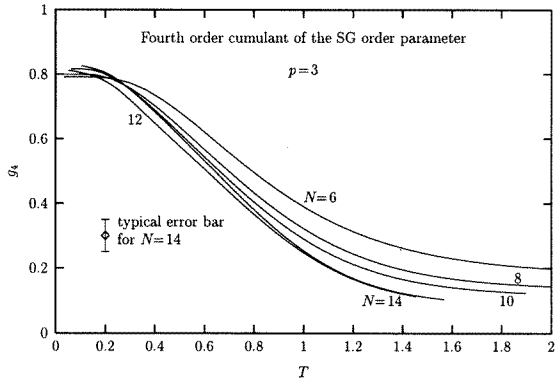

Figure 4. Order parameter cumulant plotted versus temperature for $p = 3$ and various choices of N. The error bars are about 0.1 for $N = 14$ and 0.03 for $N = 12$, but are not shown for the sake of clarity of the plot. In the case $p = 6$, the statistics of our data is even worse, and hence the corresponding data are not shown.

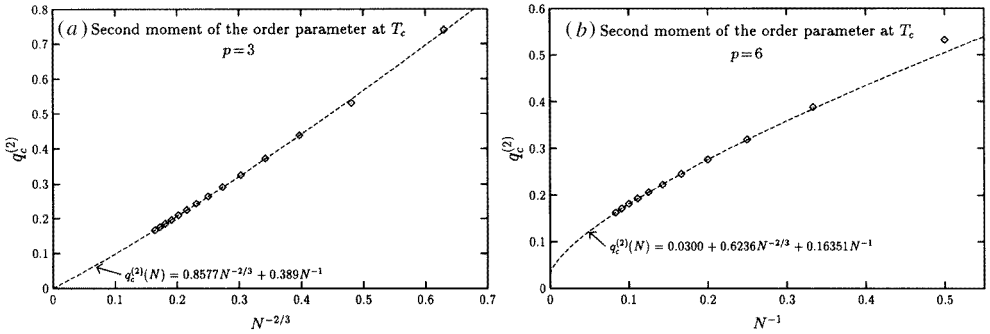

Figure 5. The plot (a) of $q^{(2)}(T_c)$ versus $N^{-2/3}$ yields estimates of $G_{(-2/3)} \approx 0.86$ and $G_{(-1)} \approx 0.4$ (cf equations (10) and (11)). In the case (b) $p = 6$, $q^{(2)}(T_c)$ as a function of N^{-1} seems to extrapolate to a finite value 0.03. This should be compared to the predicted jump in the order parameter, $q^2_{\text{jump}} = (2/15)^2 = 0.01777$ (cf equation (6)), which is quite good an agreement, in view of the inaccuracy of the extrapolation, and the fact that equation (6) is only a leading order $(p - 4)$ expansion result.

statistical errors (large fluctuations in $q^{(4)}$).

From our results it is obvious that for small N corrections to finite-size scaling are very pronounced. Although this casts doubt on the accuracy of MC studies of short-range Potts glasses, where rather small systems were used as well [14, 21], such corrections to scaling must be expected, in view of experience with the Ising mean-field spin glass [16].

Parisi *et al* [16] studied the SK model using replica field theory to obtain the following FSS relations:

$$F(T_c)/N = F_\infty + \frac{\ln N}{12N} + \frac{F_{(-1)}}{N} + \frac{F_{(-4/3)}}{N^{4/3}} + \mathrm{O}(N^{-5/3}) \tag{9}$$

$$q^{(2)}(T_c) = \frac{G_{(-2/3)}}{N^{2/3}} + \frac{G_{(-1)}}{N} + \mathrm{O}(N^{-4/3}) \tag{10}$$

which in leading order corresponds to relation (8) but contains corrections of relative order $N^{-1/3}$, and

$$U(T_c)/N = U_\infty + \frac{G_{(-2/3)}}{2N^{2/3}} + \mathrm{O}(N^{-1})\,. \tag{11}$$

The numerical values for the constants $F_{(x)}$ and $G_{(x)}$ were extracted from MC data: $G_{(-2/3)} \approx 1$, $G_{(-1)} \approx -0.02$ and $0 < -F_{(-4/3)} < F_{(-1)} \ll 1$.

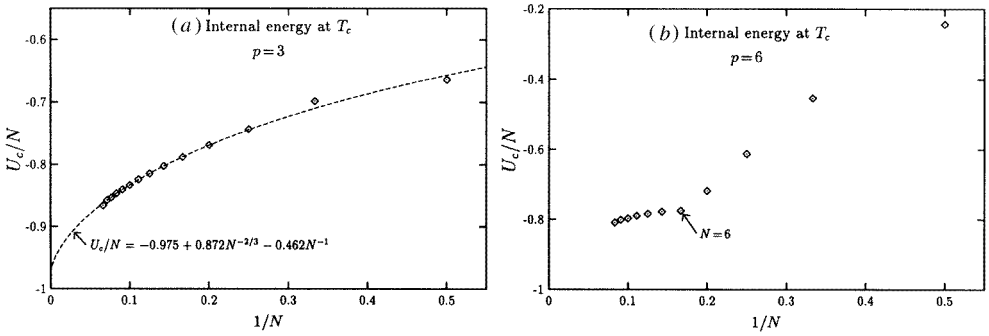

Figure 6. Plot of the internal energy $U_c/N = U(T_c)/N$ per spin versus N^{-1} at the critical point (a) for $p = 3$ and (b) $p = 6$.

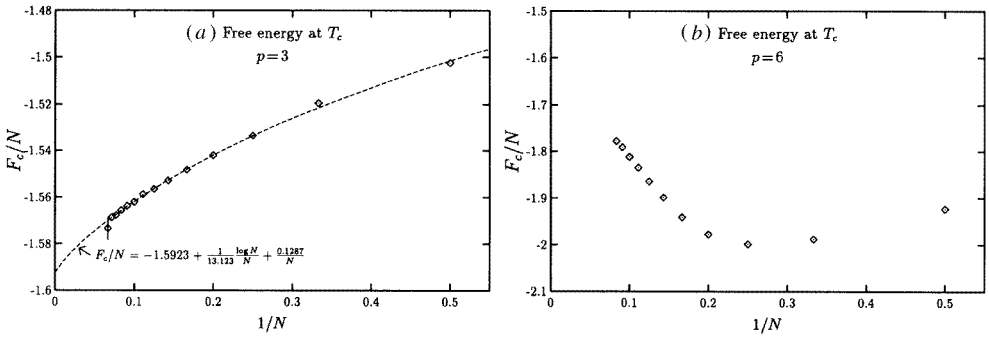

Figure 7. Plot of the free energy per spin F_c/N versus N^{-1} at the critical point (a) for $p = 3$ and (b) $p = 6$.

Trying a similar scaling for the $p = 3$ mean-field PG with bimodal bond distribution, we obtain the results shown in figures 5–7. The broken curves shown for $p = 3$ are fits to functional forms as suggested by Parisi *et al* [16]. Unfortunately, nothing is known about the coefficients, but the order of magnitude obtained from our fit looks reasonable.

Of course, the results are probably also affected by the additional phase transition at $T_2 = 0.5$. However, no clear evidence for this phase transition can be drawn from our numerical data, since the q-moments are apparently not particularly sensitive to the RCFM phase, and because our systems are, of course, rather small.

4.2. The case $p = 6$

In the case $p = 6$, it is not quite clear what kind of finite-size behaviour one should expect for such an unusual phase transition without latent heat. Mainly for comparison, we hence present our data in a similar way to the $p = 3$ case. One notes (cf figure 1) that at very high temperatures there is still a pronounced N dependence in the data, in marked contrast to the $p = 3$ case. This behaviour is easily understood in terms of the high-temperature series expansion: while for $p = 3$ we have chosen $\tilde{J}_0 = 0$, such that the coefficient of the $O(\beta)$ term in the expansion of F/N is independent of N, $\tilde{J}_0 = -3$ for $p = 6$, such that in this case the coefficient has a strong $O(N^{-1})$ contribution.

This means, however, that for $\tilde{J}_0 \neq 0$—which is necessary for the stability of the SG

phase—the system exhibits an additional strong finite-size effect unrelated to the phase transition, such that a FSS analysis of the latter will be even more difficult.

Nevertheless, a fit of $q^{(2)}$ precisely at T_c with first finite-size correction terms in $N^{-2/3}$ and N^{-1} yields reasonable agreement with our data (figure 5(*b*)). Interestingly enough, the data seem to extrapolate to a *finite* value of q_c^2 in the thermodynamic limit; this might be a hint to the finite jump in q at the transition. Of course, it is not at all obvious that a similar scaling as in the case $p = 3$ should apply here, since we deal with an unusual first-order transition here. But interpreting the lack of a latent heat as a feature of second-order transitions, it is possible that this transition still has properties in common with critical phenomena. The behaviour of the internal energy and the free energy at T_c are both not yet understood, see figures 6(*b*) and 7(*b*). It seems that these functions undergo a qualitative change in behaviour when N reaches $p = 6$.

4.3. Specific heat, energy cumulant and ferromagnetic susceptibility

For $p = 3$, the mean-field critical exponent $\alpha = 0$ precludes a power-law singularity of the specific heat, admitting only a cusp or a logarithmic singularity. Similarly, for $p = 6$, the usual delta-function singularity of $C_V(T)$ associated with a first-order transition should *not* occur since there is no latent heat involved. Indeed, there is some weak evidence that $C_V(T_c)$ converges to a finite peak for $N \to \infty$, see figures 8 and 9 and the fits in $N^{-1/3}$ and $N^{-2/3}$, which extrapolate to a maximum value of $C_V \approx 1$ for $p = 3$ and $C_V \approx 2$ for $p = 6$ in the thermodynamic limit. Again we have to add the caveat that it is not obvious that this is the appropriate scaling for $p = 6$. The peaks are rather broad, which might be related to the strong overall finite-size effect in the case $p = 6$, plus some contributions from the transition SG $\leftrightarrow$ RCFM in both cases. A high-N MC study is still necessary in order to investigate the T_2-transition.

In the case $p = 6$, the location of the maximum of C_V clearly converges to the temperature $T = T_c = 1$ (figure 10(*b*)). Conversely, for $p = 3$ we were unable to observe such a clear convergence, see figure 10(*a*). It seems that the mutual influence of the two phase transitions at T_c and T_2 is stronger for $p = 3$.

We have also calculated the energy cumulant, here defined as

$$U_4(T) = \frac{1}{2}\left(3 - \frac{[\langle \mathcal{H}^4 \rangle]}{[\langle \mathcal{H}^2 \rangle]^2}\right)$$

see figure 11. While U_4 decreases monotonically with temperature for $p = 3$, one finds

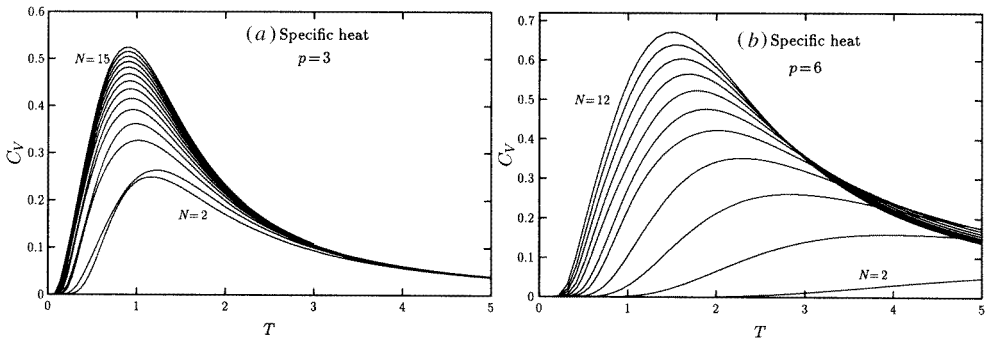

Figure 8. Specific heat per spin C_V, as a function of temperature, (*a*) for $p = 3$ and (*b*) $p = 6$.

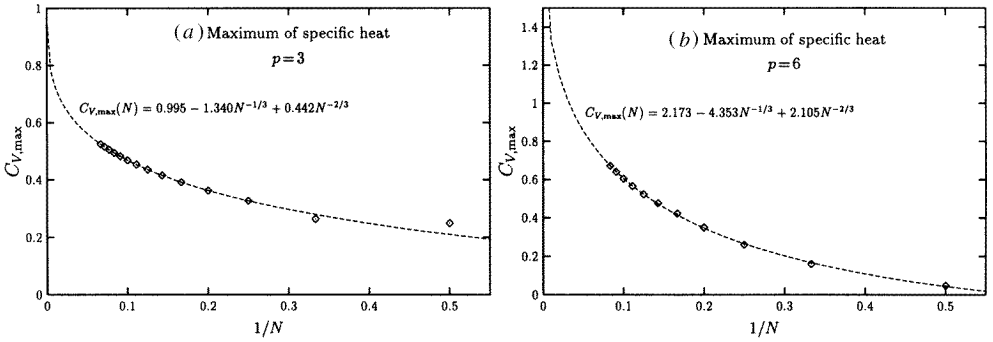

Figure 9. Maximum value of the specific heat per spin plotted versus N^{-1} (*a*) for $p = 3$ and (*b*) $p = 6$.

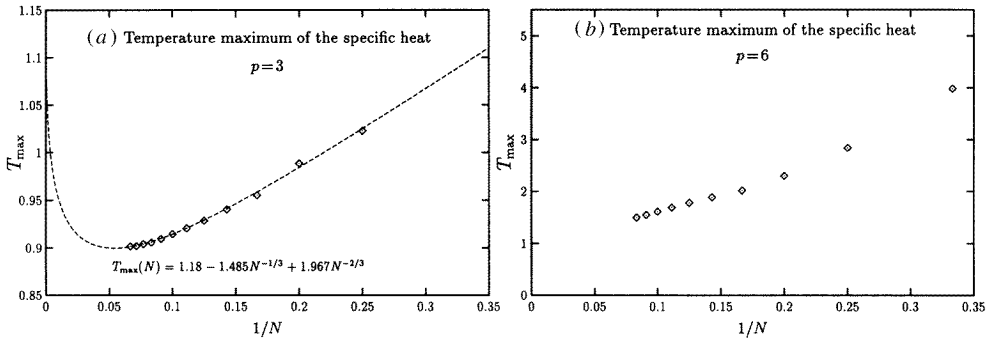

Figure 10. Location $T_{\max}$ of the specific heat maximum (*a*) for $p = 3$ and (*b*) $p = 6$ plotted versus N^{-1}. In the case of $p = 3$, a polynomial in $N^{-1/3}$ has been fitted to the data as indicated.

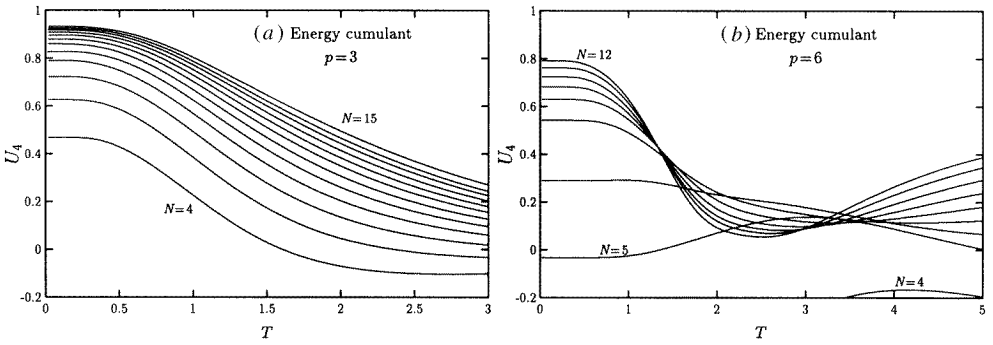

Figure 11. Energy cumulant U_4 plotted versus temperature (*a*) for $p = 3$ and (*b*) $p = 6$.

that U_4 has an intersection point and a minimum, both above T_c. However, theoretical understanding of this behaviour is still lacking. It should be mentioned that the above definition does not use centred moments and hence depends on the choice of the energy origin. It might well be that the structure observed for $p = 6$ is partly related to the non-vanishing energy value in the high-temperature limit. At any rate, one should be cautious interpreting the cumulant behaviour as a 'fingerprint' of first-order behaviour: the minimum

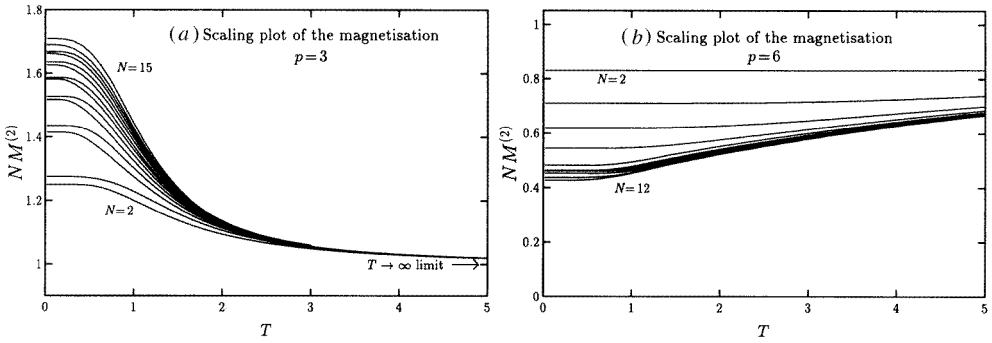

Figure 12. Normalized ferromagnetic susceptibility $T\chi_m = NM^{(2)}$ plotted versus temperature (*a*) for $p = 3$ and (*b*) $p = 6$.

which is usually observed in the cumulant near first-order transitions [22] is directly related to the presence of well separated peaks in the corresponding distribution, i.e. to the existence of a latent heat, which, however, is *not* present here.

Given the fact that at $T_2 = 0.5$ a transition to the RCFM phase occurs, the study of the ferromagnetic susceptibility $T\chi_M \equiv N[\langle m^2\rangle] \equiv NM^{(2)}$ is also of interest. (Note that for every single bond configuration $\langle\vec{m}\rangle \equiv 0$, due to the Potts symmetry.) While for $p = 3$ this quantity increases with decreasing T, but seems to converge to finite values for $N \to \infty$ everywhere, for $p = 6$ this quantity even decreases with decreasing temperature (figure 12).

4.4. The ground state

Since the finite-size behaviour at $T = 0$ is not known, we plotted our results for U_0, S_0, $M_0^{(2)}$ and $q_0^{(2)}$ versus N^{-1} and tried an empirical fitting with the most promising exponent in N, see figure 13. (U_0 and S_0 are the ground-state energy and entropy, respectively, while $M_0^{(2)}$ and $q_0^{(2)}$ are the second moments of the magnetization and the SG order parameter at $T = 0$.)

For $p = 3$, we observed weak even–odd oscillations, whereas in the case $p = 6$ the phenomena are more complicated and inhibit a reliable extrapolation of our data to $N^{-1} = 0$. The data points are then aligned on arcs from $N = 2$ to 6, and from 6 to 12. Hence, data points for $N = 13$ and 14 could indicate the trend of the system sizes up to $N = 18$, but their calculation would require memory of up to two Gigabytes, which was inaccessible to us.

It is theoretically not clear whether the ground-state entropy S_0 should vanish. We found an upper limit of $S_0/N(p = 3) < 0.01$ and $S_0/N(p = 6) < 0.1$. Our estimates for the ground-state energy are $U_0/N = -1.30(5)$ for $p = 3$ and $U_0/N = -1.3(2)$ for $p = 6$. A high-p estimator of U_0 for the PG with *Gaussian* bond distribution is $-\sqrt{p \ln p}$ [6]; this is not confirmed by our 'bimodal' data.

The behaviour of the magnetization (or its second moment $M^{(2)}$) indicates some evidence for a finite but very small value of the ground-state magnetization M_0 in the case $p = 3$, whereas M_0 vanishes clearly in the case $p = 6$ (cf figure 13).

The spin-glass order parameter remains finite for $T \to 0$ in both cases, as expected. We obtain $q_0^{(2)} = 0.45(5)$ in the case $p = 3$, and $q_0^{(2)} = 0.17(4)$ for $p = 6$.

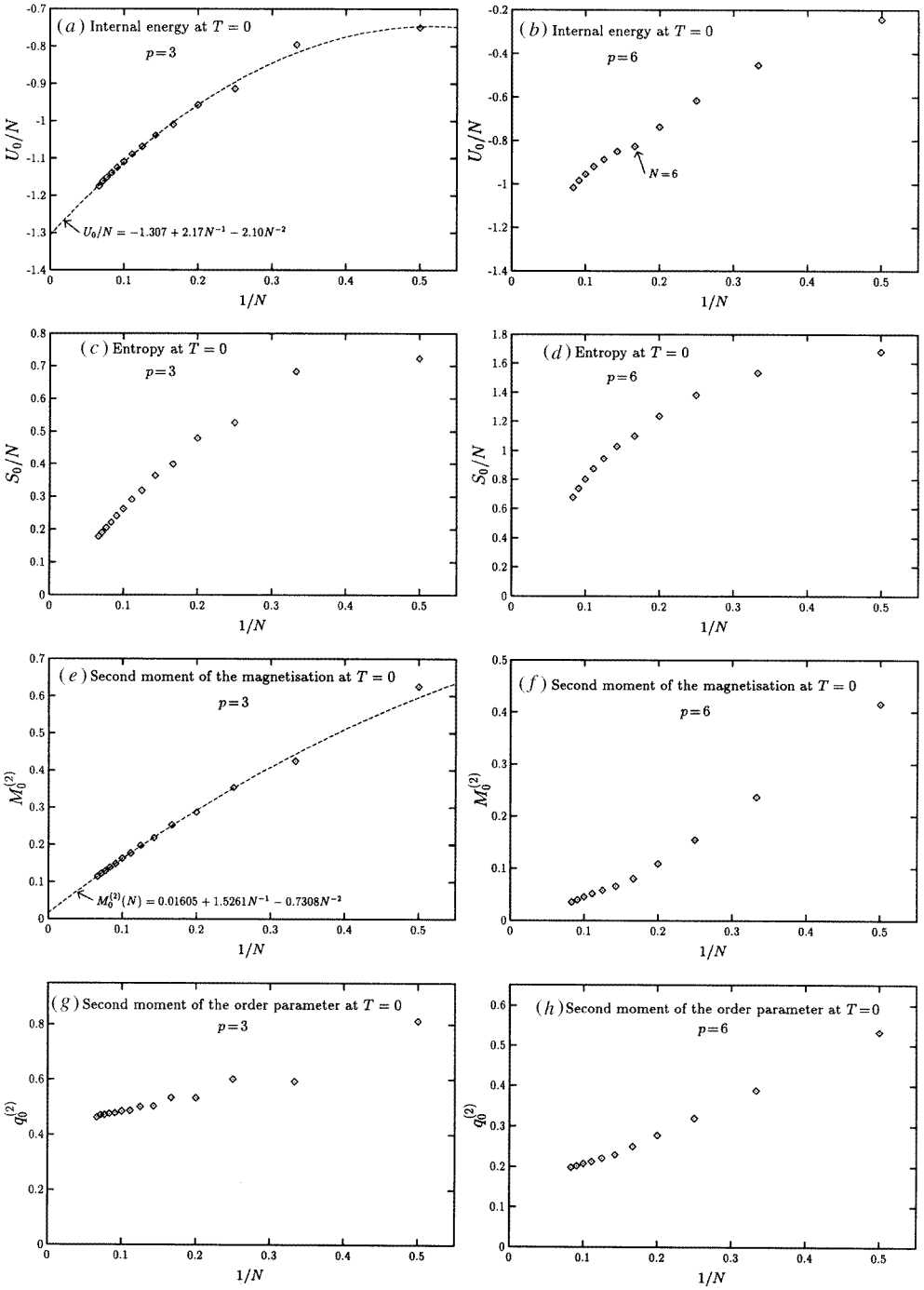

Figure 13. Ground state ($T = 0$) observables plotted versus N^{-1}: internal energy per spin U_0/N (*a*) for $p = 3$ and (*b*) $p = 6$, entropy per spin S_0/N (*c*) for $p = 3$ and (*d*) $p = 6$, the second moment of the magnetization $M_0^{(2)}$ (*e*) for $p = 3$ and (*f*) $p = 6$, and the second moment of the SG order parameter $q_0^{(2)}$ (*g*) for $p = 3$ and (*h*) $p = 6$.

5. Summary and discussion

The exact statistical mechanics approach to the $p = 3$ Potts glass gives first ideas about the ground state and confirms that the FSS results of Parisi *et al* [16] for the SK model apply qualitatively also to the present model for $p = 3$. In the case $p = 6$, the calculation of data for slightly bigger systems than $N = 12$ is still desirable to get more reliable results. Any clear evidence for the first-order character of the transition at $p = 6$ is lacking from our data. In more detail, we can summarize our results as follows:

- From our data, we are not able to identify clearly whether there is some ferromagnetic ordering or not at $T = 0$, and a vanishing ground-state entropy, related to a number of ground states which, at most, increases slower than exponentially with N. The ground-state energy is estimated by us as $U_0/N(p = 3) = -1.30(5)$ and $U_0/N(p = 6) = -1.3(2)$ in units of $\tilde{J}$. An upper limit for the ground-state entropy is $S_0/N < 0.01$ for $p = 3$ and $S_0/N < 0.1$ for $p = 6$, while both data sets are well compatible with $S_0 = 0$.
- There is some rather weak evidence for a small non-zero magnetization at $T = 0$ in the case $p = 3$, whereas the magnetization vanishes for $p = 6$. But even for $p = 3$ a zero magnetization is not definitively ruled out.
- The spin-glass order parameter is, as expected, in both cases clearly positive for all $T < T_c$. Thus our extrapolations give clear evidence for the existence of a spin-glass phase.
- The nature of the RCFM phase is not clear, like the transition into it. In particular, there is no evidence for a divergent ferromagnetic susceptibility: for $p = 6$, it even decreases with decreasing temperature.
- The specific heat behaviour is compatible with a non-divergent singularity at the transition(s).
- In the case $p = 6$ there are, in addition to finite-size effects associated with the transitions, additional finite-size effects related to the necessary antiferromagnetic bias of the bond distribution, as revealed by the leading-order terms of the high-temperature series expansion.
- Although the systems are too small to draw any firm conclusions, the data are compatible with a finite jump in q for $p = 6$, which, by order of magnitude, agrees with the analytic prediction, equation (6). For $p = 3$, the corresponding extrapolation indicates a vanishing jump, in agreement with the known second-order behaviour. The hysteresis-like behaviour of the order parameter, which should occur in the first-order case $p > 4$ in a temperature interval $T_c < T < T_A$ [7, 10, 11], can show up in the present approach at most only indirectly via the finite-size behaviour of the order parameter distribution: In the thermodynamic limit, our procedure should converge to the equilibrium jump without hysteresis ($q^{(k)}$ is a single-valued function of T for all N), while for finite N all metastable states also contribute to the averages. However, the finite-size behaviour of the distribution function near a first-order spin-glass transition without latent heat is, to our knowledge, unknown (in marked contrast to first-order transitions in pure systems, where a well established theory and methodology [37] exists). Therefore, it is unclear how to extract the contributions from the metastable states from the finite-size data. This lack of theoretical understanding has of course also affected our extrapolations, for which we simply used the same powers of N as in the second-order case, without any deeper justification.
- Results for larger values of N could possibly be achieved with the help of modern Monte Carlo methods like simulated tempering [38]. The free-energy behaviour obtained in

the present study for small systems could be used as an educated guess for the necessary reweighting schemes.

We hope that we have been able to show that the mean-field Potts glass still poses many challenging questions.

Acknowledgments

We acknowledge partial support from the Deutsche Forschungsgemeinschaft, Sonderforschungsbereich 262/D1. BOP would like to thank the Regionales Hochschulrechenzentrum Kaiserslautern for generous allocation of Cray time, and the Zentralinstitut für Angewandte Mathematik, Jülich, for technical support and advice. Moreover, we would like to thank H Flyvbjerg for a careful reading of the manuscript.

References

[1] Binder K and Young A P 1986 *Rev. Mod. Phys.* **58** 801
[2] Fischer K H and Hertz J 1991 *Spin Glasses* (Cambridge: Cambridge University Press)
[3] Mezard M, Parisi G and Virasoro M 1987 *Spin Glass Theory and Beyond* (Singapore: World Scientific)
[4] Stein D S 1992 *Spin Glasses and Biology* (Singapore: World Scientific)
[5] Elderfield D and Sherrington D 1983 *J. Phys. C: Solid State Phys.* **16** L497, L971, L1169
[6] Gross D J, Kanter I and Sompolinsky H 1985 *Phys. Rev. Lett.* **55** 304
[7] Cwilich G and Kirkpatrick T R 1989 *J. Phys. A: Math. Gen.* **22** 4971
[8] Cwilich G 1990 *J. Phys. A: Math. Gen.* **23** 5029
[9] Binder K and Reger J D 1992 *Adv. Phys.* **41** 547
[10] Kirkpatrick T R and Wolynes P G 1987 *Phys. Rev.* B **35** 3072; **36** 8552
[11] Kirkpatrick T R and Thirumalai D 1987 *Phys. Rev.* B **36** 5388; **37** 5342
Thirumalai D and Kirkpatrick T R 1988 *Phys. Rev.* B **38** 4881
[12] Götze W and Sjögren L 1992 *Rep. Prog. Phys.* **55** 241
[13] Schreider G and Reger J D 1995 *J. Physique* to appear
[14] Scheucher M and Reger J D 1993 *Z. Phys.* B **91** 383
[15] Young A P and Kirkpatrick S 1982 *Phys. Rev.* B **25** 440
[16] Parisi G, Ritort F and Slanina F 1993 *J. Phys. A: Math. Gen.* **26** 247, 3775
[17] Zia R K P and Wallace D J 1975 *J. Phys. A: Math. Gen.* **8** 1495
[18] Scheucher M and Reger J D 1992 *Phys. Rev.* B **45** 2499
[19] Scheucher M, Reger J D, Binder K and Young A P 1991 *Europhys. Lett.* **14** 119
[20] Scheucher M, Reger J D and Young A P 1992 *Europhys. Lett.* **20** 343
[21] Scheucher M, Reger J D, Binder K and Young A P 1990 *Phys. Rev.* B **42** 6881
[22] Vollmayr K, Reger J D, Scheucher M and Binder K 1993 *Z. Phys.* B **91** 113
[23] Parisi G 1979 *Phys. Rev. Lett.* **43** 1754; 1980 *J. Phys. A: Math. Gen.* **13** 1101
[24] Binder K and Heermann D W 1988 *Monte Carlo Simulation in Statistical Physics—an Introduction* (Berlin: Springer)
[25] Binder K 1992 Finite size effects at phase transitions *Computational Methods in Field Theory* ed H Gausterer and C B Lang (Berlin: Springer)
[26] Parisi G and Ritort F 1993 *J. Phys. A: Math. Gen.* **26** 6711
Ciria J C, Parisi G and Ritort F 1993 *J. Phys. A: Math. Gen.* **26** 6731
[27] Ferrenberg A M and Swendsen R H 1989 *Phys. Rev. Lett.* **63** 1195
[28] Harary F and Palmer E 1973 *Graphical Enumeration* (London: Academic)
[29] Sherrington D and Kirkpatrick S 1975 *Phys. Rev. Lett.* **35** 1792
[30] Edwards S F and Anderson P W 1975 *J. Phys. F: Met. Phys.* **5** L49
[31] Suzuki M 1977 *Prog. Theor. Phys.* **58** 1151
[32] Binder K 1981 *Z. Phys.* B **43** 119
[33] Bhatt R N and Young A P 1986 *J. Magn. Magn. Mater.* **54–57** 191
[34] Bhatt R N and Young A P 1985 *Phys. Rev. Lett.* **54** 924
[35] Young A P 1983 *Phys. Rev. Lett.* **51** 1206
[36] Bhatt R N and Young A P 1988 *Phys. Rev.* B **37** 5606

[37] Janke W 1994 *Computer Simulation Studies in Condensed Matter Physics* vol 7, ed D P Landau, K K Mon and H B Schüttler (Berlin: Springer)
[38] Marinari E and Parisi G 1992 *Europhys. Lett.* **19** 451